

*Short Communication*

## Enhancement of Titanium Alloy Corrosion Resistance via Anodic Oxidation Treatment

Hong Jiang

School of Materials Science and Engineering, University of Shanghai for Science and Technology,  
No.516,Jungong Road, Yangpu District,Shanghai,200093, P.R. China  
E-mail: [jianghongvivi@tom.com](mailto:jianghongvivi@tom.com)

Received: 27 November 2017 / Accepted: 18 January 2018 / Published: 6 March 2018

The present work presented the electrochemical treatment of anodic oxidation of TA6V alloy and pure titanium, along with the evaluation of the passivity currents of the TA6V alloy treated under varying conditions. The test electrolyte used in the anodic oxidation was a chromic acid (CA) solution with and without the addition of hydrofluoric acid (HF). On the anodized samples, the passivity current was remarkably decreased, and the range of passive potentials was increased.

**Keywords:** Anodic oxidation; Titanium alloy; Corrosion resistance; Chronoamperometry; Potentiostatic test

### 1. INTRODUCTION

Titanium alloys (esp. Ti6Al4V) have gained wide application in the orthopaedic fields as biomaterials, as they are compatible with human tissue, highly resistant to localized and generalized corrosion, and possess desirable mechanical features (esp. fatigue resistance) [1-3]. These desirable properties occur because the thin oxide surface layer (thickness: 1.5–10 nm) that is naturally formed on the titanium metal surface when exposed to air at ambient temperature provides remarkable biocompatibility, along with the benefits brought by the commercially pure titanium (cp-Ti) implants during manufacturing [4-6]. The bone tissue is directly in contact with the surface oxide film instead of the Ti bulk metal; thus, the desirable Ti implant biocompatibility possibly lies in the features of the above oxide layer. To study the osseointegration between bone tissue and the implant, it is necessary to investigate the surface features of this film [7-9]. Thereby, the aims of a majority of studies on the tissue reactions to implant surfaces have involved the modification of the thin film surface roughness. Many techniques have been proposed to roughen the surfaces, including plasma spraying, blasting, sintering and etching [10-14]. In recent years, other methods have been reported for the development

of new surfaces, including sol gel processing [15], anodic plasma-chemical treatment [16], anodic oxidation under galvanostatic [17-20] and potentiostatic modes [21, 22] and ion implantation [23].

Some oxides with different crystalline structures have been formed, as Ti has highly affinity to oxygen.  $\text{TiO}_2$ , as a thermodynamically stable oxide formed in natural atmosphere, is available in the following three crystalline structures: anatase, brookite and rutile [24]. Generally, the first structure is formed via anodic oxidation, and the last one is obtained via anodic oxidation and then a thermal treatment [25-39]. The technique used in forming the oxide layer determines the oxide surface and the surface morphology, both of which affect the interaction between the implant and the environment [40-42]. The colour variation of the oxide generated via anodic oxidation indicates the film thickness. The nature of the electrolyte and the anodization process determine, to a large extent, the relation of oxide thickness with colour [17]. The coloration of the titanium oxide surface is altered if the above parameters vary in any way. According to the preparation of surface oxide by Sul et al. [17], several factors influence the electrochemical growth performance of the oxide film on cp-Ti metal, including the surface area ratio of cathode to anode, agitation speed, given temperature, anodic forming voltage, applied current density, electrolyte concentration, etc.

To optimize the biocompatibility of the implant surface, the Ti surface has been chemically and physically treated through different methods. It was observed that the methods contributing to the roughness enhancement of the surface and the formation of a  $\text{TiO}_2$  layer on the surface promoted the biological behaviour of the implants [20]. Favourable results were obtained after P and Ca ions were incorporated into the surface layer in the formation of films [43]. In the present work, we studied the electrochemical conditions of the growth of anodic oxide films on titanium and TA6V alloy surfaces in chromic acid (CA) with and without the addition of fluoride.

## 2. EXPERIMENTS

The  $1.5 \times 1.5 \text{ cm}^2$  samples were mechanically polished using a diamond paste ( $1/4 \mu\text{m}$ ), followed by ultrasonic rinsing and then anodization, where the surface was chemically modified through the polishing treatment. Table 1 shows the compositions of the electrolyte and the species that most likely existed in the solution, as shown in the Pourbaix-computed concentration-pH diagrams. In CA, in the absence of HF (CA), a compact film was formed due to anodization, while in the electrolyte of CA/HF, the formation of porous films was observed.

**Table 1.** Electrolyte composition.

Name	$\text{CrO}_3$ (M)	HF (M)
CA	0.5	0
CA+HF	0.5	0.01

A conventional three-electrode configuration was used for voltammetric measurements, where the counter and reference electrodes were a platinum electrode and a saturated calomel electrode

(SCE), respectively, as shown in potentiodynamic I–V curves. These measurements were carried out under no-stirring and no-aeration conditions. The potential of the working electrode was increased constantly from 0 mV to 4000 mV at a rate of 2000 mV/h.

The electrochemically obtained titanium oxide films are characterized by peculiar optical properties. They are perfectly transparent but acquire particular colours due to interference effects resulting from multiple reflections of light between the external and internal surfaces of the film.

A two-electrode geometry was used for the chrono-amperometric experiments, where the counter electrode was titanium, with the results are shown in I–t curves. The determination of the procedure and arrangement was based on the industrial anodization procedure: the voltage between a titanium cathode and the sample was increased in five equal steps of 1 min each, up to the final voltage of 12, 20, 60 or 100 V. After continuous measurement, the obtained current density was described as a function of time, and the calculation of the electric charge exchange in varying steps was based on it. Characterizations were also carried out by directly jumping to the final voltage.

Conventional potentiodynamic measurements and long-time passivity current experiments were carried out for the characterization of sample corrosion features. All the experiments were carried out at 38 °C in a buffered physiological solution consisting of 0.06 g/L NaH<sub>2</sub>PO<sub>4</sub>, 0.06 g/L Na<sub>2</sub>HPO<sub>4</sub>, 0.35 g/L NaHCO<sub>3</sub>, and 8.74 g/L NaCl.

To obtain the passivity currents at a potential that titanium alloys normally display under this circumstance, potentiostatic experiments were specifically carried out. After grinding using emery paper up to 4000 mesh and then oxidization under air or anodization with one of the aforementioned electrochemical techniques, the samples were inserted in a 5 l cell filled with deaerated physiological solution. Continuous deaeration of the solution was carried out throughout the experiments via N<sub>2</sub> bubbling. A titanium wire was covered with a PTFE insulating coating and spot welded to each sample so as to be electrically connected to the experimental devices. The strips were placed on a PTFE support. Simultaneously, potentiostatic experiments were carried out on 11 samples that were connected in parallel to the working channel of the potentiostat. The symmetrical position of these samples was obtained by placing the counter electrode in the cell centre to ensure that the current could be uniformly distributed.

### 3. RESULTS AND DISCUSSION

As shown in Figure 1, the electrochemical property of TA6V and Ti 40 in two types of medium was displayed using potential-dynamic curves, where the general shapes were comparable. In brief, when the applied potential was in a range of 0 to 100 mV, the anodic current was significantly increased, as the surface and cell system was stabilized, and the current reached a plateau at 1000 to 2500 mV. These two materials showed almost the same performance in electrolyte CA without fluorination, where a rapidly obtained constant current remained extremely insignificant till beyond 2500 mV.

It was observed that the anodic current density increased remarkably after HF was added into the solution. Tests in the presence of electrolytes with different contents of HF were also carried out,

which showed an increase in the maximum current density of TA6V. A very small increase in the current density was observed at higher voltages, although no generalized or localized corrosion was observed on the specimens at the end of the tests. The difference may lie in the different parameters used during the experiments, including the temperature, agitation of the electrolyte, and so on, which, to a large extent, determined the growth and dissolution mechanism.

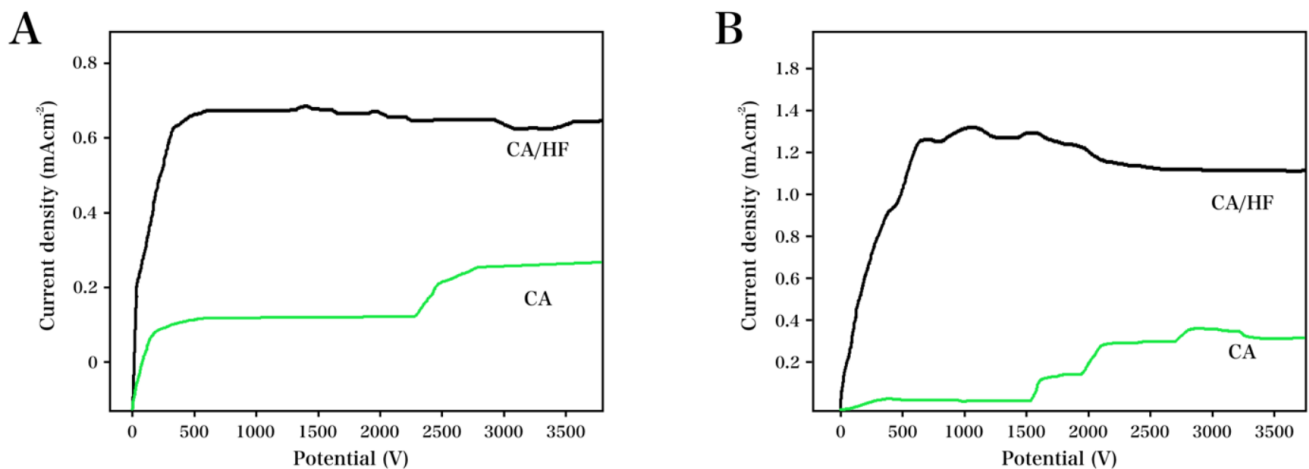


**Figure 1.** (A) Anodic polarisation curves recorded for Ti 40 in CA and in CA/HF electrolyte. (B) Anodic polarisation curves recorded for TA6V in CA and in CA/HF electrolyte.

The current densities recorded for the TA6V and Ti 40 alloys after anodization in  $\text{CrO}_3$  solution in the absence of fluoride under varying constant voltages are shown in Figure 2. A high initial current density was observed, possibly due to the control of the constant voltage source. This phenomenon was commonly observed at Ti based alloys [44, 45]. The current density vs. time curves showed an abrupt and drastic decrease within the initial seconds and then different shapes, depending, to a large extent, on the voltage. A rapid current decrease down to an extremely low value was observed when the voltage was low, at 2 and 5 V, suggesting the low voltage cannot trigger the effective anodization [46, 47]. When the applied voltage was of a more moderate level, the current decreased to a value that could not be neglected and subsequently either slowly dropped, as in the tests at 12 and 20 V using TA6V, or remained constant till the test was completed. For the specimens with thicker oxide films, the range of the potential with current density comparable to the minimum sensitivity of the experimental instrumentation was approximately 12 V higher for the specimens anodized at high current density than for those anodized at low current density. When the voltage was at a high level, a minimum value was observed at 60 V (with TA6V) and at 12 and 20 V (with Ti 40), and the current increased as a function of time.

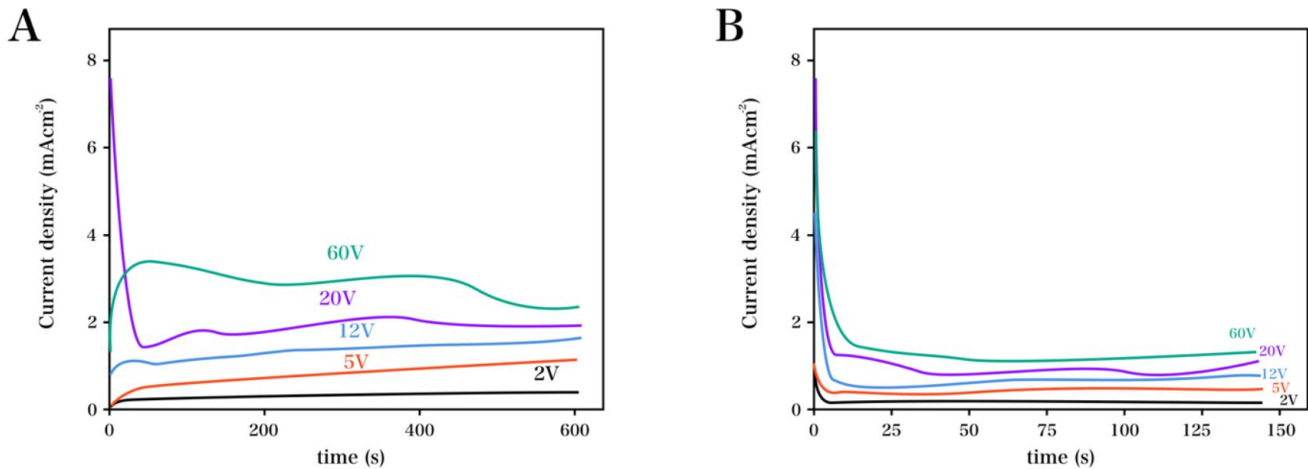


**Figure 2.** (A) Chrono-amperometric characterization of Ti 40 in CA electrolyte at varying voltages.(B) Chrono-amperometric characterization of TA6V in CA electrolyte at varying voltages.

The curves recorded for the electrolyte after the addition of HF were totally different from the classical ones, as shown in Figure 3. In brief, the current remained at almost 0 A or slowly increased to a value that could not be neglected when the voltage was low, suggesting the anodization process is very weak [48, 49]. A rapid decrease in the current was observed within the initial seconds, reaching a constant value for Ti 40 (at a middle level of voltage) and for TA6V (at other voltages). Fluorine is incorporated into the films grown from a fluorinated electrolyte, and small quantities of vanadium are present on the film grown on the TA6V substrates. In addition, a minimum current value was observed, and finally, a remarkable and constant maximum value was obtained.

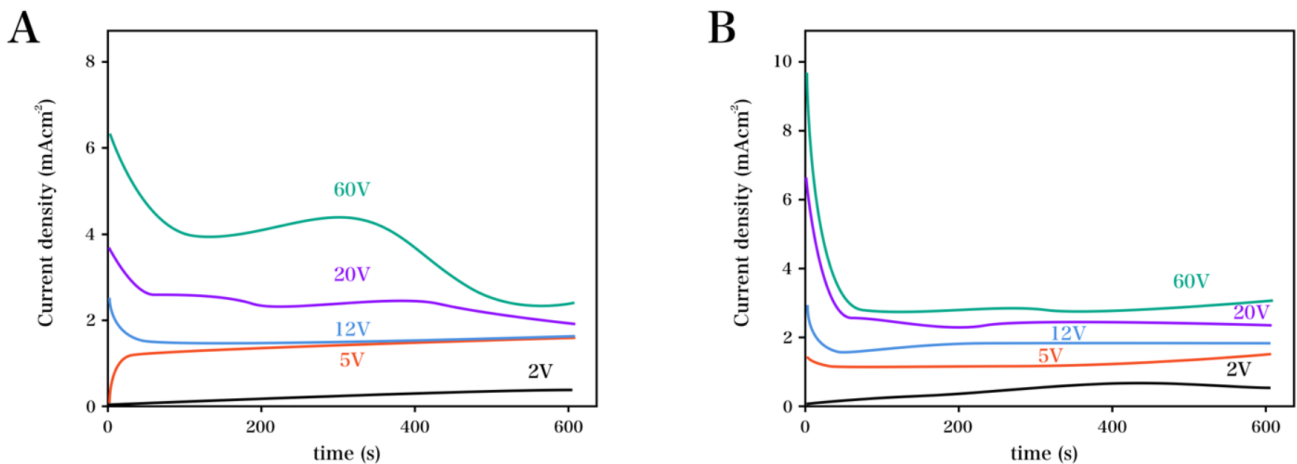


**Figure 3.** (A) Chrono-amperometric characterization of Ti 40 in CA/HF electrolyte at varying voltages. (B) Chrono-amperometric characterization of TA6V in CA/HF electrolyte at varying voltages.

The potentiostatic test results are presented in Figure 4. The calculation was based on the smoothing method on five sample measurements after oxidization at 5 V, 12 V, 20 V and 60 V. For each sample, the mean value and the standard deviation of the passivity current density was obtained at 600 to 825 h, with the results displayed in Figure 5.

Compared with the samples after air oxidization and CA anodization, the samples treated after anodization in CA/HF showed a dramatically lower passivity current density. Under semi-stationary conditions, the ratio is *ca.* 1:10 and 1:5, respectively. When the transitory period was considered, the ratio was much higher. Compared with the anodization in CA/HF, the anodization in CA showed a significantly higher standard deviation, as the film was more porous. This can be attributed to a modification of the structure of the compact anodic film and, more precisely, to a breakdown phenomenon.

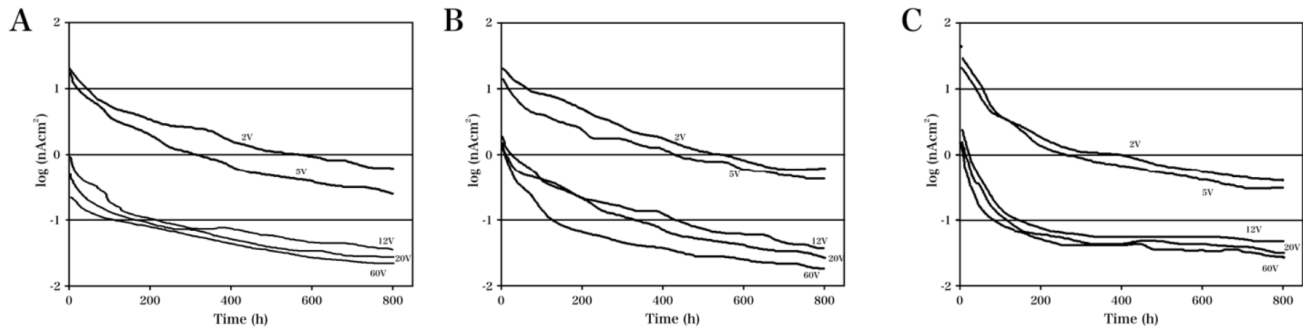


**Figure 4.** (A) Potentiostatic experiments in physiological solution on TA6V samples after air oxidization. (B) Potentiostatic experiments in physiological solution on TA6V samples after oxidization in CA electrolyte. (C) Potentiostatic experiments in physiological solution on TA6V samples oxidized in CA/HF electrolyte.

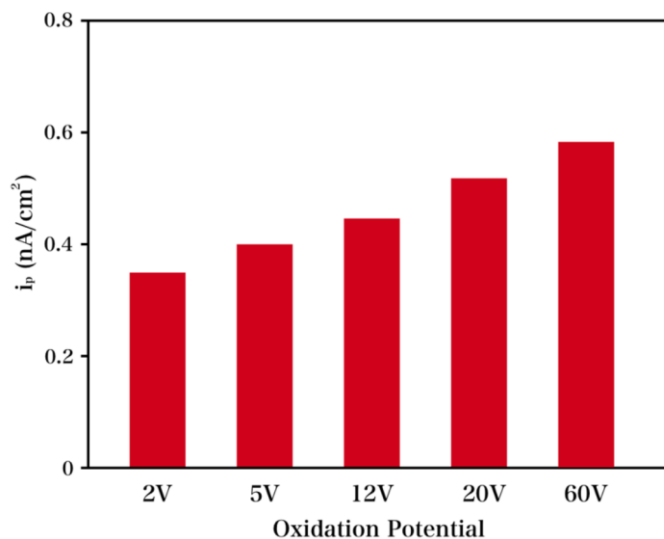


**Figure 5.** Average passivity currents and standard deviations in physiological solution of TA6V samples, after oxidization and anodization under varying conditions.

The thicknesses of the oxide films treated after CA/HF anodization varied slightly among these samples. As the thickness was increased, a decrease in the passivity current density was observed for all cases, whereas an increase was found in the standard deviation of the results. The samples treated with high current density anodization and low current density anodization showed no remarkable variation between each other. For compact anodization in CA electrolyte, a breakdown of the film provokes a definitive perturbation of the growth process. Measuring the dependence of the passivity

current drop on the thickness of the anodization was essential, and the knowledge could be used to enhance the biocompatibility of titanium alloys for further orthopaedic applications. It is expected that the electrical resistance increased as the oxide film grew thicker. A thicker layer of passivation film could further enhance the biocompatibility [50, 51]. Based on the report of Zitter and Plenk [52], it was hypothesized that the anodized titanium showed a more favourable performance compared with that treated by spontaneous oxidization in air or conventional passivity techniques. The step height measurements, confirmed by chemical analysis of the electrolyte after anodization, prove that an important dissolution of the substrate occurs during the experiment. The galvanic elements that possibly led to the redox reactions of the metallic surface, even in the case of no corrosion, would not be formed in the presence of a practically insulative oxide.

#### 4. CONCLUSIONS

In the present work, we presented the electrochemical properties of TA6V and titanium alloys in CA electrolyte with and without the addition of fluorine species, along with the structural and physio-chemical investigation, which enabled the growth process of the anodic films to be successfully and precisely described. In our case, the release of metallic ions was remarkably decreased, which lowered the risks of local irritation or long-term sensitization, as the metallic ions were diffused into the surrounding tissues.

#### ACKNOWLEDGEMENTS

This work was supported by grants from Shanghai natural science fund project(13ZR1427900): Energy nickel base alloy pipe hot extrusion process of organization evolution simulation studies.

#### References

1. M. Shokouhfar, C. Dehghanian, M. Montazeri and A. Baradaran, *Applied Surface Science*, 258 (2012) 2416.
2. L.T. Duarte, S.R. Biaggio, R.C. Rocha-Filho and N. Bocchi, *Corrosion Science*, 72 (2013) 35.
3. M. Fazel, H. Salimjazi and M. Golozar, *Applied Surface Science*, 324 (2015) 751.
4. L. Benea, E. Mardare-Danaila, M. Mardare and J.-P. Celis, *Corrosion Science*, 80 (2014) 331.
5. W. Simka, M. Sowa, R.P. Socha, A. Maciej and J. Michalska, *Electrochimica Acta*, 104 (2013) 518.
6. M. Jamesh, S. Kumar and T.S.N.S. Narayanan, *Journal of materials engineering and performance*, 21 (2012) 900.
7. C. Moseke, F. Hage, E. Vorndran and U. Gbureck, *Applied Surface Science*, 258 (2012) 5399.
8. E.M. Szesz, B.L. Pereira, N.K. Kuromoto, C.E. Marino, G.B. de Souza and P. Soares, *Thin Solid Films*, 528 (2013) 163.
9. M. Sowa, K. Greń, A.I. Kukharenko, D.M. Korotin, J. Michalska, L. Szyk-Warszyńska, M. Mosiałek, J. Żak, E. Pamuła and E.Z. Kurmaev, *Materials Science and Engineering: C*, 42 (2014) 529.
10. Y.T. Sul, C.B. Johansson, Y. Kang, D.G. Jeon and T. Albrektsson, *Clinical implant dentistry and related research*, 4 (2002) 78.
11. K.B. Kim, B.C. Kim, S.J. Ha and M.W. Cho, *Journal of Mechanical Science and Technology*, 31 (2017) 4387.
12. A. Maciej, J. Michalska, W. Simka and R. Socha, *Ochrona przed Korozją*, (2015) 400.

13. H.-g. Wang and Y.-p. Song, *Surface Technology*, 6 (2015) 005.
14. X. Lu, X. Feng, Y. Zuo, C. Zheng, S. Lu and L. Xu, *Surface and Coatings Technology*, 270 (2015) 227.
15. D. Velten, V. Biehl, F. Aubertin, B. Valeske, W. Possart and J. Breme, *Journal of Biomedical Materials Research Part A*, 59 (2002) 18.
16. V. Frauchiger, F. Schlottig, B. Gasser and M. Textor, *Biomaterials*, 25 (2004) 593.
17. Y.-T. Sul, C.B. Johansson, Y. Jeong and T. Albrektsson, *Medical engineering & physics*, 23 (2001) 329.
18. Y.-T. Sul, C.B. Johansson, S. Petronis, A. Krozer, Y. Jeong, A. Wennerberg and T. Albrektsson, *Biomaterials*, 23 (2002) 491.
19. Y.-T. Sul, *Biomaterials*, 24 (2003) 3893.
20. Y. Sul, C. Johansson, Y. Jeong, K. Röser, A. Wennerberg and T. Albrektsson, *Journal of Materials Science: Materials in Medicine*, 12 (2001) 1025.
21. M. Kawashita, X.-Y. Cui, H.M. Kim, T. Kokubo and T. Nakamura, Bonelike apatite formation on anodically oxidized titanium metal in simulated body fluid, *Key Engineering Materials*, Trans Tech Publ, 2004, pp. 459.
22. T.Y. Xiong, X.-Y. Cui, H.M. Kim, M. Kawashita, T. Kokubo, J. Wu, H.-Z. Jin and T. Nakamura, Effect of surface morphology and crystal structure on bioactivity of titania films formed on titanium metal via anodic oxidation in sulfuric acid solution, *Key Engineering Materials*, Trans Tech Publ, 2004, pp. 375.
23. Y.-T. Sul, C.B. Johansson and T. Albrektsson, *International Journal of Oral & Maxillofacial Implants*, 17 (2002)
24. B. Yang, M. Uchida, H.-M. Kim, X. Zhang and T. Kokubo, *Biomaterials*, 25 (2004) 1003.
25. C.-K. Lee, *Materials Science and Engineering: B*, 177 (2012) 810.
26. J. Xing, Z. Xia, J. Hu, Y. Zhang and L. Zhong, *Corrosion Science*, 75 (2013) 212.
27. K. Korkmaz, *Surface and Coatings Technology*, 272 (2015) 72.
28. N. Movahedi and A. Habibolahzadeh, *Materials Letters*, 164 (2016) 558.
29. L.J. Zhou, F. Wang, C. Yang, W.W. Zhang, Z.Y. Xiao and Y.Y. Li, *Materials & Design*, 78 (2015) 25.
30. S.A. Nikolaev, E.V. Golubina and M.I. Shilina, *Applied Catalysis B: Environmental*, 208 (2017) 116.
31. M.A. Vasylyev, S.P. Chenakin and L.F. Yatsenko, *Acta Materialia*, 103 (2016) 761.
32. S.-N. Pak, Z. Jiang, Z. Yao, J.-M. Ju, K.-S. Ju and U.-J. Pak, *Surface and Coatings Technology*, 325 (2017) 579.
33. W. Tu, Y. Cheng, T. Zhan, J. Han and Y. Cheng, *Int. J. Electrochem. Sci*, 12 (2017) 10863.
34. F. Yan, X. Wang, X. Wang, X. Li and C. Wang, *Int. J. Electrochem. Sci*, 12 (2017) 11212.
35. P. Zhang and X. Guo, *Corrosion Science*, 91 (2015) 101.
36. H.-H. Yang, X.-S. Wang, Y.-M. Wang, Y.-L. Wang and Z.-H. Zhang, *Materials*, 10 (2017) 609.
37. Y.A.N. Zhiyu, W. Xin, S.U.N. Bing, W.E.N. Mi and H.A.N. Yue, *Plasma Science and Technology*, 19 (2017) 035501.
38. M. Kaseem, J.H. Kwon and Y.G. Ko, *RSC Advances*, 6 (2016) 107109.
39. Z. Zhan, L.I. Jingyang, D. Jianxin and Y.A.O. Zhihao, *Journal of Chinese Society for Corrosion and protection*, 37 (2017) 1.
40. V.A. Barão, M.T. Mathew, W.G. Assunção, J.C.C. Yuan, M.A. Wimmer and C. Sukotjo, *Clinical oral implants research*, 23 (2012) 1055.
41. L. Benea, E. Danaila and P. Ponthiaux, *Corrosion Science*, 91 (2015) 262.
42. M. Sandhyarani, N. Rameshbabu, K. Venkateswarlu, D. Sreekanth and C. Subrahmanyam, *Journal of Alloys and Compounds*, 553 (2013) 324.
43. L.-H. Li, Y.-M. Kong, H.-W. Kim, Y.-W. Kim, H.-E. Kim, S.-J. Heo and J.-Y. Koak, *Biomaterials*, 25 (2004) 2867.

44. L. Fu, K. Xie, H. Zhang, Y. Zheng, W. Su and Z. Liu, *Coatings*, 7 (2017) 232.
45. A. Wang, C. Wang, L. Fu, W. Wong-Ng and Y. Lan, *Nano-Micro Letters*, 9 (2017) 47.
46. S. Ozkan, A. Mazare and P. Schmuki, *Electrochemistry Communications*, 65 (2016) 18.
47. R. Sánchez-Tovar, R.M. Fernández-Domene, A. Martínez-Sánchez, E. Blasco-Tamarit and J. García-Antón, *Journal of Catalysis*, 330 (2015) 434.
48. M. Iraj, M. Kolahdouz, E. Asl-Soleimani, E. Esmaeili and Z. Kolahdouz, *Journal of Materials Science: Materials in Electronics*, 27 (2016) 6496.
49. T. Kondo, S. Nagao, T. Yanagishita, N.T. Nguyen, K. Lee, P. Schmuki and H. Masuda, *Electrochemistry Communications*, 50 (2015) 73.
50. S.L.M. Ribeiro Filho, C.H. Lauro, A.H.S. Bueno and L.C. Brandão, *Arabian Journal for Science and Engineering*, 41 (2016) 4313.
51. A.T. Sidambe, I. Todd and P.V. Hatton, *Powder Metallurgy*, 59 (2016) 57.
52. H. Zitter and H. Plenk, *Journal of Biomedical Materials Research Part A*, 21 (1987) 881

© 2018 The Authors. Published by ESG ([www.electrochemsci.org](http://www.electrochemsci.org)). This article is an open access article distributed under the terms and conditions of the Creative Commons Attribution license (<http://creativecommons.org/licenses/by/4.0/>).